One-Pot Sol-Gel Synthesis of Highly Insulative Hybrid P(AAm-Co-AAc)-Silica Aerogels with Improved Mechanical and Thermal Properties

Akshay A. Ransing , Rushikesh P. Dhavale , Vinayak G. Parale , Uzma K.H. Bangi , Haryeong Choi , Wonjun Lee , Jiseung Kim , Qi Wang , Varsha D. Phadtare , Taehee Kim , Wook Ki Jung , Hyung-Ho Park *

Posted Date: 19 July 2023

doi: 10.20944/preprints202307.1321.v1

Keywords: One-pot sol-gel synthesis; Hybrid P(AAm-CO-AAc)-silica aerogel; Epoxy ring-opening polymerization; Thermal stability; Mechanical properties

Article

One-Pot Sol-Gel Synthesis of Highly Insulative Hybrid P(AAm-Co-AAc)-Silica Aerogels with Improved Mechanical and Thermal Properties

Akshay A. Ransing [1], Rushikesh P. Dhavale [1], Vinayak G. Parale [1], Uzma K. H. Bangi [2], Haryeong Choi [1], Wonjun Lee [1], Jiseung Kim [1], Qi Wang [1], Varsha D. Phadtare [1], Taehee Kim [1], Wook Ki Jung [3] and Hyung-Ho Park [1,*]

[1] Department of Materials Science and Engineering, Yonsei University, Seoul 03722, Republic of Korea
[2] Department of Physics, School of Physical Sciences, Punyashlok Ahilyadevi Holkar Solapur University, Solapur—Pune National Highway, Kegaon, Solapur 413 255, Maharashtra, India
[3] Agency for Defense Development (ADD), Daejeon 34146, Republic of Korea
* Correspondence: hhpark@yonsei.ac.kr

Abstract: Silica aerogels and their derivatives have outstanding thermal properties with exceptional values in the thermal insulation industry. However, the brittle nature restricts its large-scale commercialization. Thus, enhancing their mechanical strength without affecting their thermal insulating properties is essential. Therefore, for the first time, highly thermally stable Poly(acrylamide-Co-acrylic acid) partial sodium salt is used as a reinforcing polymer to synthesize hybrid P(AAm-CO-AAc)-silica aerogels via epoxy ring-opening polymerization in the present study. Functional groups in P(AAm-CO-AAc) partial sodium salts, such as $CONH_2$ and COOH, acted as nucleophiles for the epoxy ring-opening reaction with (3-glycidyloxypropyl)trimethoxysilane, which resulted in a seven-fold enhancement in mechanical strength compared to that of a pristine silica aerogel while maintaining the thermal conductivity at less than 30.6 mW/mK and porosity of more than 93.68%. Moreover, the hybrid P(AAm-CO-AAc)-silica aerogel demonstrated improved thermal stability up to 343 ^{0}C owing to the synergetic effect between P(AAm-CO-AAc) and the silica aerogel, corresponding to thermal stability and strong covalent bonding among them. These excellent results illustrate that this new synthetic approach for producing hybrid P(AAm-CO-AAc)-silica aerogels is useful for enhancing the mechanical strength of a pristine silica aerogel without impairing its thermal insulating property and shows potential as an industrial heat insulation material.

Keywords: one-pot sol-gel synthesis; hybrid P(AAm-CO-AAc)-silica aerogel; epoxy ring-opening polymerization; thermal stability; mechanical properties

1. Introduction

In recent years, the heat insulation industry has paid a great deal of attention to silica aerogels due to their noteworthy properties, such as very low density (0.03–0.1 g/cm^3), high porosity (90–99%), high specific surface area (100-1000 m^2/g), and low thermal conductivity (0.02–0.044 W/mK) [1–5]. Moreover, their fascinating properties make them suitable for a wide range of applications in the aerospace and other industries, including sensors, building construction, super-insulated windows, and energy storage devices [6–12]. However, besides the outstanding properties of silica aerogels, their brittle and fragile nature constrains their long-term and practicability for heat insulation. Therefore, to overcome these shortcomings of silica aerogels, researchers are currently focused on enhancing their mechanical strength without affecting their intrinsic properties [13–15].

Until now, several methods have been explored to overcome this strengthening problem, such as aging, surface modification, co-precursors methods, as well as organic polymers and fibers for synthesizing hybrid or composite reinforced silica aerogels [16–20]. Considering feasible and worthwhile ways to enhance the structural strength of silica aerogel, several researchers have recently tried

 doi:10.20944/preprints202307.1321.v1

to focus on synthesizing hybrid organic-inorganic silica aerogels in which different organic or synthetic polymers are crosslinked with the silica aerogel using various crosslinkers. For instance, polyurea, epoxides, polyacrylates, polyimides, and polystyrene polymers have been crosslinked with pristine silica aerogel by using diisocyanates, (3-aminopropyl) triethoxysilane, acrylates, anhydrides, vinyl trimethoxysilane, among others, as the crosslinker, respectively [13,21–26]. Two different strategies have mainly been used to incorporate organic polymers as structural reinforcing agents into the silica framework. One is the post-gelation washing method whereby a solid silica gel network is immersed in a 10 to 15-fold higher volume solution of the selected polymer to react with the active surface functional groups of silica for structural strengthening [27]. Another is the one-pot synthesis method whereby a predetermined amount of the selected polymer is added to the silica sol before gelation occurs, which allows the polymer to react not only with active the surface functional groups of silica but also inside the bulk part to strengthen the silica gel network [28]. Moreover, the amount of polymer solution used for the synthesis makes a considerable difference to the large-scale production cost of aerogels. considering that latter method is obviously more efficient for synthesizing hybrid polymer-silica aerogel compared to the post-gelation washing. Thus, preparing hybrid silica aerogel using different organic polymers via a cost-effective one-pot sol-gel synthesis method is an efficient approach [14]. However, enhancing chemical crosslinking with organic polymers causes an interruption in the pore structure of the pristine silica aerogel, which is unfavorable for maintaining a high surface area, low density, and high porosity. It also creates a solid path for heat flow through it, which mainly affects the ultralow thermal conductivity and high thermal stability of silica aerogel and thereby limits their applicability.

In this investigation, we reported a one-pot sol-gel synthesis of hybrid Poly(acrylamide-Co-acrylic acid)-silica aerogel (TGP_X aerogel) via epoxy ring-opening polymerization with enhanced thermal stability and mechanical properties of a pristine silica aerogel. To the best of our knowledge, for the first time P(AAm-CO-AAc) is used as a crosslinking polymer to enhance the mechanical strength of a pristine silica aerogel. In the present study, organic-inorganic hybrid aerogels were prepared by adding P(AAm-CO-AAc) to tetramethyl orthosilicate (TMOS) silica precursor with (3-glycidyloxypropyl)trimethoxysilane (GPTMS) as a crosslinking agent via epoxy ring-opening polymerization and supercritical alcohol drying. The high thermal stability of P(AAm-CO-AAc) compared to other available organic polymers provides a great advantage for the field of heat insulation [29]. Moreover, the amide and carboxylic functionalities of P(AAm-CO-AAc) allow it to react with the epoxy groups of GPTMS to form covalent bonds via epoxy polymerization, which enhances the structural strength of the hybrid silica aerogel. Furthermore, the effect of P(AAm-CO-AAc) (PACA) wt% variation on the physical, chemical, structural, thermal, and mechanical properties of the hybrid TGP_X (X denotes wt% of the polymer) aerogels were investigated and reported.

2. Results and Discussion

The thermal properties of the hybrid aerogels were investigated by assessing the passage of thermal energy through the material, which occurs via three different mechanisms: solid conductivity, gaseous conductivity, and radiative conductivity [30,31]. When it comes to heat flow through a porous aerogel material, one must consider various factors such as porosity, pore size, density, and the type of material used in the synthesis, all of which can significantly impact the heat transfer properties of the aerogel. Thus, carefully analyzing and understanding these factors is crucial for synthetic optimization since. While controlling these parameters, the mechanical properties of aerogels can be deprived. On the other hand, organic-inorganic hybridization generally enhances the mechanical properties such as the brittleness of an inorganic aerogel, which leads to suppresses the thermal properties of inorganic aerogel. Hence, to overcome these drawbacks and enhance the mechanical properties of a silica aerogel without affecting its thermal properties, we strategically used the highly thermally stable PACA polymer as a crosslinking polymer, which can covalently bond with the silica aerogel as well as help to control the thermal properties of silica aerogel. The possible reaction mechanism during the sol-gel synthesis of the TGP_X aerogels via *in situ* epoxy ring-opening polymerization is illustrated in Scheme 1. Here, epoxy ring-opening polymerization is performed by using the

Preprints (www.preprints.org) | NOT PEER-REVIEWED | Posted: 19 July 2023 doi:10.20944/preprints202307.1321.v1

epoxy group of GPTMS and the COOH and $CONH_2$ groups of PACA polymer; where, COOH and $CONH_2$ groups act as a nucleophile, and donate a pair of electrons for the epoxy ring-opening polymerization process [32,33], which improves the structural strength of the TGP_X aerogels by forming strong covalent bonds between GPTMS and PACA polymer. In addition, hydroxyl groups formed due to the epoxy ring-opening of GPTMS also allow a further condensation reaction with the hydrolyzed TMOS precursor. In addition to the siloxane bonding, the strong covalent bonds formed by the epoxy ring-opening polymerization between GPTMS and PACA impart crack-free hybrid TGP_X aerogel monoliths. Increasing the wt% of PACA leads to complete structural crosslinking and provides improved mechanical strength, as determined by the increase in the compression modulus values of the hybrid TGP_X aerogels compared to a pristine silica aerogel. Unlike that seen in other organic-inorganic hybrid aerogels, the high thermal stability and low thermal conductivity of PACA polymer can restrict structural heat conduction through the solid part of the TGP_X aerogel, which could maintain the thermal conductivity and more importantly enhance the thermal stability compared to a pristine silica aerogel. Thus, hybrid TGP_X aerogels are prepared with variation of PACA (wt%) and its impact on the mechanical and thermal properties was studied.

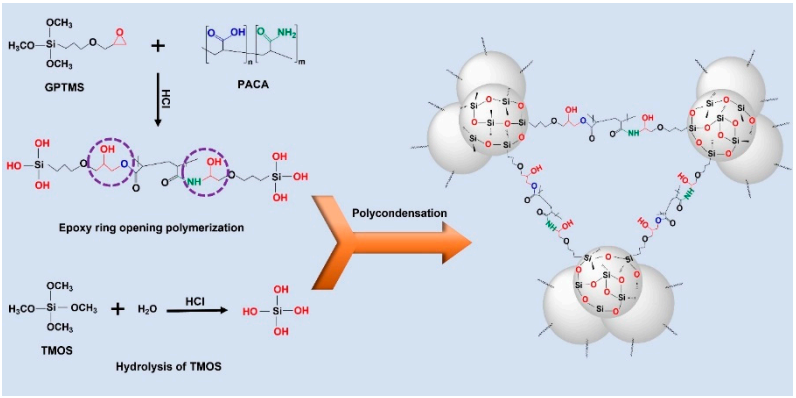

Scheme 1. The reaction mechanism in the one-pot sol-gel synthesis of hybrid TGP_X aerogels.

2.1. The Bonding Mechanism of TGP_X Aerogels

2.1.1. Fourier-Transform Infrared (FTIR) Analysis of the TGP_X Aerogels

To probe bonding mechanism of TGP_X aerogels with varying PACA polymer wt%, the FTIR spectra of the TGP_X aerogels are carried out and depicted in Figure 1. The predominant absorption peaks occurring at 1060, 800, and 445 cm^{-1} are attributed to the Si-O-Si asymmetric and symmetric stretching, and deformation vibrations, respectively [34–36]. The vibrational peaks at 1400, 2860, and 2946 cm^{-1} correspond to C-H deformation, C-H symmetric stretching, and asymmetric stretching, respectively, arising from GPTMS and PACA polymers [37]. Vibration peaks at 1736 and 1212 cm^{-1} associated with the C=O and C-N groups can be seen in the FTIR spectra of all of the samples except for TGP_0 aerogel sample, which confirms the presence of PACA polymer. Moreover, peak intensity of C=O increased with increasing wt% of PACA in the rest of the hybrid TGP_X samples [38,39]. The FTIR spectrum of crosslinked hybrid TGP_X aerogels showed the broad and small vibrational peak at around 3400 cm^{-1} corresponds to the -OH group compared to the TGP_0 aerogel, which further confirms the consumption of formed hydroxyl groups due to the epoxy ring-opening of GPTMS through the reaction with the TMOS precursor. Thus, the FTIR spectrum of the TGP_X aerogels with varying PACA polymer wt% verify the bonding mechanism of PACA in hybrid TGP_X aerogels.

Preprints (www.preprints.org) | NOT PEER-REVIEWED | Posted: 19 July 2023 doi:10.20944/preprints202307.1321.v1

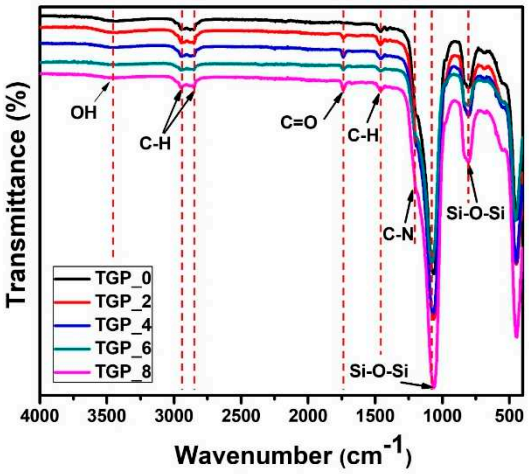

Figure 1. FTIR spectra of the TGP_X aerogels with varying PACA concentration.

2.1.2. X-ray Photoelectron Spectroscopy (XPS) Analysis of the TGP_X Aerogels

The XPS spectra showcased in Figure 2 offer significant insight into the surface elemental composition of the TGP_0 and TGP_8 aerogels, which is crucial for understanding the epoxy ring-opening polymerization process. The XPS survey scan spectra confirm the presence of the Si, C, N, and O elements in the TGP_0 and TGP_8 aerogels (Figure 2a). The high-resolution XPS of Si 2p spectra in Figure 2b exhibit distinct peaks at 101.8 and 102.5 eV for the TGP_0 aerogel and 101.9 and 103.3 eV for the TGP_8 aerogel corresponding to Si-C and Si-O bonds, respectively; where Si-O bonds indicate the presence of Si(IV) chemical state [40,41]. Likewise, Figure 2c provides a clear visualization of the high-resolution O 1s spectra, revealing distinct peaks of the XPS peak for TGP_0 aerogels located at 531.5 and 532.2 eV, which confirm the presence of Si-OH and O-Si bonds. Similarly, for TGP_8 aerogel, the peak at 531.7 eV and 532.4 eV are indicative of Si-OH and O-Si bonding respectively [42,43]. It is worth noting that these spectra are obtained from both GPTMS and TMOS precursors, providing substantial evidence to support the presence of Si-O-Si siloxane bonding in hybrid TGP_8 aerogels. Furthermore, the high-resolution XPS spectrum of the C 1s for TGP_0 aerogel in Figure 2d is deconvoluted into two peaks at 284.5 eV and 286.1 eV corresponding to the C-C and C-O bonds, respectively, with measured peak area component ratio of 1: 2 for C-C : C-O, where C-O bonds confirms that the TGP_0 aerogel had undergone epoxy ring surface modification [44]. Comparatively, the high-resolution XPS of C 1s spectrum of TGP_8 aerogel sample deconvoluted into three peaks at 284.5, 286.2, and 288.5 eV associated with C-C, C-O, and C=O bonds, respectively, with measured peak area component ratio C-C: C-O: C=O of 6: 3: 1, as tabulated in inset of Figure 2d [45–47]. A significant increase in the peak area for C-C bonds and a profound decrease in the peak area of C-O bonds are indicative of the epoxy ring-opening polymerization between GPTMS and PACA. Furthermore, the presence of C=O bonds and N atoms (the inset in Figure 2a) from PACA confirmed the use of COOH and $CONH_2$ groups as nucleophiles in the epoxy ring-opening reaction. [46]. Therefore, these observations from XPS analysis results confirm the successful formation of hybrid TGP_X aerogels via *in situ* epoxy ring-opening polymerization.

Preprints (www.preprints.org) | NOT PEER-REVIEWED | Posted: 19 July 2023 doi:10.20944/preprints202307.1321.v1

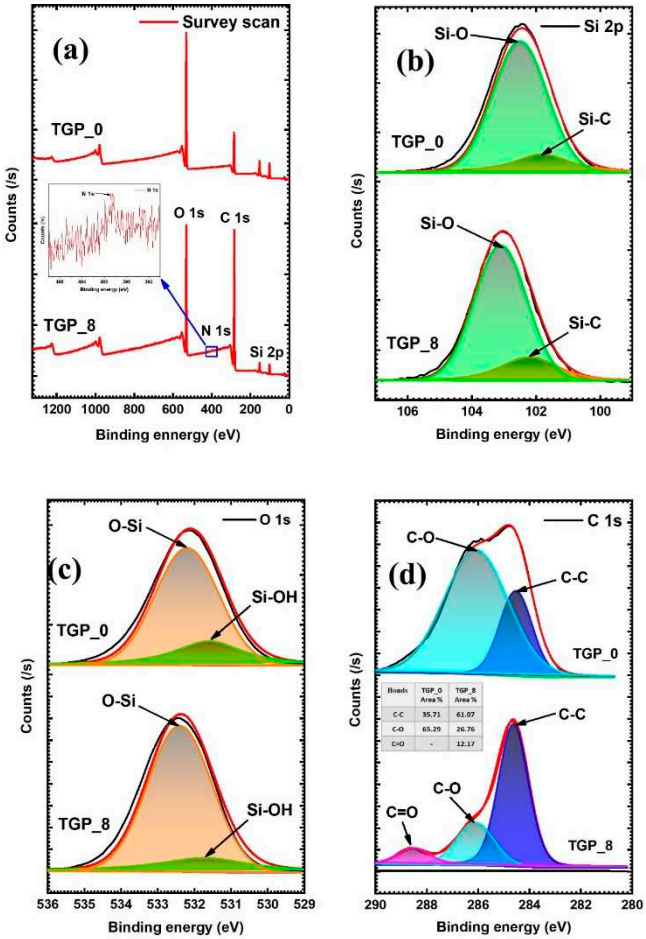

Figure 2. XPS analysis of (a) survey scan spectra and high-resolution (b) Si 2p, (c) O 1s, and (d) C 1s spectra of the TGP_0 and hybrid TGP_8 aerogels.

2.2. Physical Property and Textural Analysis of the TGP_X Aerogels

Thermal conductivity and thermal stability are the two most crucial parameters to assess the thermal insulation properties of an aerogel. While, the thermal conductivity and stability of porous aerogels principally subjected to heat transfer through the solid phase, gas phase, and radiation, which are mainly influenced by the density and porosity of the material [48]. Therefore, the physical properties of hybrid TGP_X aerogels with varying PACA polymer (0 to 8 wt%) in terms of density, porosity, thermal conductivity, specific surface area, pore volume, and average pore diameter are measured and summarized in Table 1. As expected, very small and monotonous increases in the bulk density and thermal conductivity values of the TGP_X crosslinked aerogels were observed with increasing PACA concentration. Wherein, bulk densities of TGP_X crosslinked aerogels increased from 0.084 to 0.12 cm^3/g due to the addition of molecularly dense PACA polymer. While the porosities% of TGP_X aerogel, calculated by using Equation (1) decreased from 95.57% to 93.68%:

$$\text{Porosity } (\%) = [1 - (\varrho b/\varrho s)] \times 100, \quad (1)$$

where ϱb is the bulk density and ϱs is the skeletal density (~1.9 g/cc) [36]. This predictable decrease in porosity is due to the interruption in the pore structure of TGP_X aerogel caused by cross-linking. Moreover, the increase in thermal conductivity from 22.4 to 30.6 mW/mK can be attributed to cross-linking between GPTMS and PACA polymer, which generating heat transfer passages due to the increase in density and decrease in porosity with increasing PACA concentration [49]. In general,, the addition of organic content to a silica aerogel leads to an increase in thermal conductivity. For example, Ghica et al. [50] observed an increase in thermal conductivity from 31.3 to 85.4 mW/mK after the

Preprints (www.preprints.org) | NOT PEER-REVIEWED | Posted: 19 July 2023 doi:10.20944/preprints202307.1321.v1

reinforcement of a silica aerogel with optimized polyamide pulps. Moreover, Merillas et al. [51] analyzed that, the synthesized polyurethane-reinforced silica composite aerogel that exhibited enhanced thermal conductivity from 33.4 to 52.5 mW/mK. Similarly, Ilhan et al. [52] and Hae-Noo-Ree Jung et al. [53] reported improved thermal conductivity of hydrophobic silica aerogels to around 41 and 131 mW/mK with the addition of polystyrene and poly(methyl methacrylate), respectively. These results confirm that the addition of an organic polymer drastic increase in thermal conductivity of the hybrid aerogel. Hence, the thermal conductivity values of the TGP_X aerogels in the present work from 22.4 to 30.6 mW/mK are comparable to those of these previously reported organic-inorganic hybrid aerogels [36,50–53] owing to the synergy among the thermally less conductive PACA polymer (60 mW/mK) [54] and the silica aerogel.

Nitrogen adsorption-desorption isotherms were obtained for the TGP_X aerogels; the corresponding Brunauer-Emmett-Teller (BET) and Barrette-Joyner-Halenda (BJH) plots for specific surface area and pore size distribution are shown at Figures 3a and 4b, respectively. All the isotherms shown in Figure 3a belong to type IV curves and H3-type hysteresis, indicating mesoporous structure of the TGP_X aerogels. The specific surface area of TGP_X aerogel decreased bit-by-bit from 608.6 to 369.0 m^2/g with increasing PACA polymer wt%. Correspondingly, pore volume decreased from 1.01 to 0.60 cm^3/g, as obtained from the BJH pore size distribution curves shown in Figure 3b. Moreover, the average pore diameters were found in the range of 6.44–7.38 nm, which confirms the mesoporous structure of TGP_X aerogels. The results above clearly demonstrate that the specific surface area and pore volume decrease with an increase in the wt% of PACA polymer in TGP_X aerogel. Thus, it is evident that the epoxy crosslinking polymerization induces the shrinkage and deformation in the pore size, which resulted in decrease in specific surface area and pore volume of hybrid TGP_X aerogels.

Table 1. The physical properties of the TGP_X aerogels with varying PACA concentration.

Aerogel	Density (g/cm^3)	Porosity (%)	Thermal Conductivity (mW/mK)	S_{BET} (m^2/g)	Pore Volume (cm^3/g)	Average Pore Diameter (nm)
TGP_0	0.084	95.57	22.4	608.6	1.01	6.65
TGP_2	0.087	95.42	22.8	552.4	0.89	6.44
TGP_4	0.096	94.94	23.9	493.9	0.82	6.65
TGP_6	0.10	94.73	24.5	456.8	0.75	6.60
TGP_8	0.12	93.68	30.6	369.0	0.60	7.38

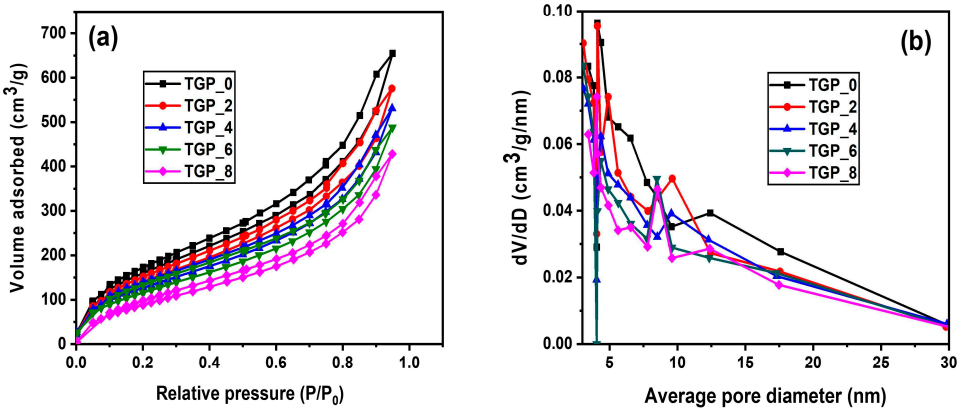

 doi:10.20944/preprints202307.1321.v1

Figure 3. (a) Nitrogen adsorption-desorption isotherms and (b) the average pore size distribution of the TGP_X aerogels with varying PACA concentration.

2.3. Morphological Analysis of the TGP_X Aerogels

The surface morphologies and reduction in average particle sizes of the TGP_X aerogels with PACA polymer wt% were observed through FESEM analysis, as shown in Figure 4a–o. Figure 4a,b show FESEM images of the TGP_0 aerogel at different magnifications, which clearly exhibit aggregated secondary silica particles having an average particle size of ~116 nm (Figure 4c) with a highly porous structure. However, the FESEM images and histograms of average particle size distribution of the hybrid TGP_X aerogels with varying PACA polymer concentration (2 to 8 wt%) shown in Figure 4d–o demonstrate interconnected silica particles forming a uniform mesoporous network with decreasing average particle size. Moreover, the observed decrease in average particle size from 116 nm (TGP_0) to 63 nm (TGP_8) with increasing PACA concentration owing to constraints induced by PACA on the growth of the silica particles. Increased epoxy polymer crosslinking with increasing PACA polymer wt% reinforces the structural strength of the hybrid TGP_X aerogels and forms crack-free and robust silica aerogels (the images in the insets of Figure 4a,d,g,j,m). In addition, the uniform mesoporous distribution provides a tortuous path for heat conduction, which effectively restricts heat transfer through the aerogel, thereby successfully bestowing thermal insulating capability of hybrid TGP_X aerogel successfully.

Preprints (www.preprints.org) | NOT PEER-REVIEWED | Posted: 19 July 2023 doi:10.20944/preprints202307.1321.v1

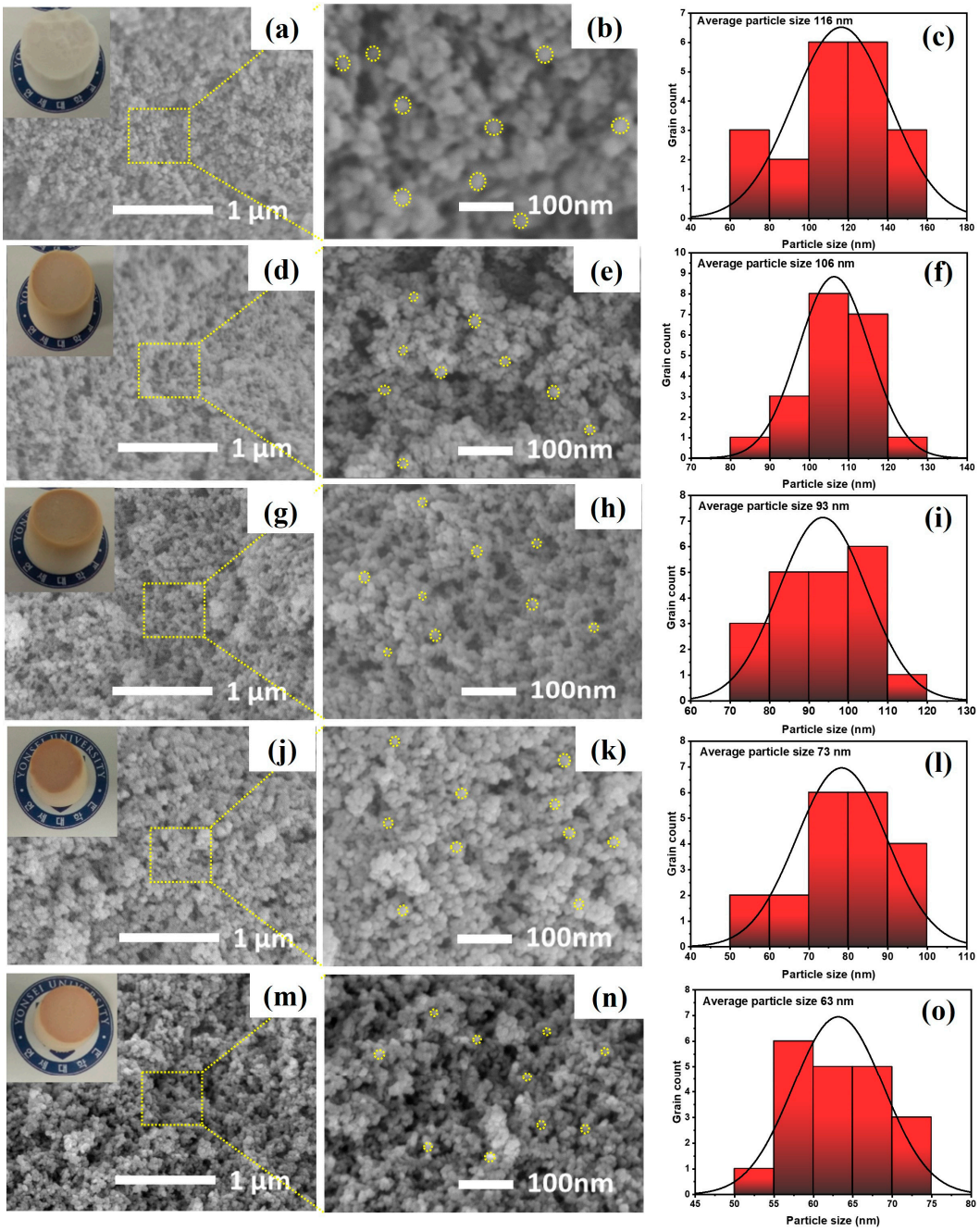

Figure 4. FESEM images with inset photographs and particle distribution plots of the TGP_X aerogels with varying PACA concentration: (a–c) TGP_0, (d–f) TGP_2, (g–i) TGP_4, (j–l) TGP_6, and (m–o) TGP_8 aerogels.

2.4. Mechanical Property Analysis of the TGP_X Aerogels

The industrial applicability of silica aerogel recommends that it should be mechanically strong enough and hold out against large compressive loads. However, synthesizing hybrid silica aerogel is one of the most effective approaches to getting mechanically strong aerogel, which makes it able to survive with higher compressive load. The mechanical properties of the TGP_X aerogels were measured by using a compressive strength measurement (Shimadzu, Japan, AGX-50kNVD) under the compressive load. The compression stress-strain curves of the TGP_X aerogels with varying PACA concentration are shown in Figure 5 to investigate the mechanical properties. The compression stress of the TGP_X aerogels increases linearly from 0.16 to 0.76 MPa with increased crosslinking polymerization between GPTMS and PACA concentration compared to the pristine TGP_0 aerogel. Hence,

Preprints (www.preprints.org) | NOT PEER-REVIEWED | Posted: 19 July 2023 doi:10.20944/preprints202307.1321.v1

the compression modulus of the TGP_X aerogels increased from 0.4 MPa for the pristine TGP_0 aerogel to 2.9 MPa for the PACA hybridized TGP_8 aerogel (Table 2). It is observed that the compression modulus of the TGP_X aerogels enhanced with increasing the PACA concentration due to the augmented epoxy ring-opening polymerization. Moreover, a minute increase in compression stress led to minimal changes in the compression modulus of the TGP_6 and TGP_8 aerogels, which suggests saturation and completed epoxy ring-opening polymerization in hybrid TGP_X aerogels.

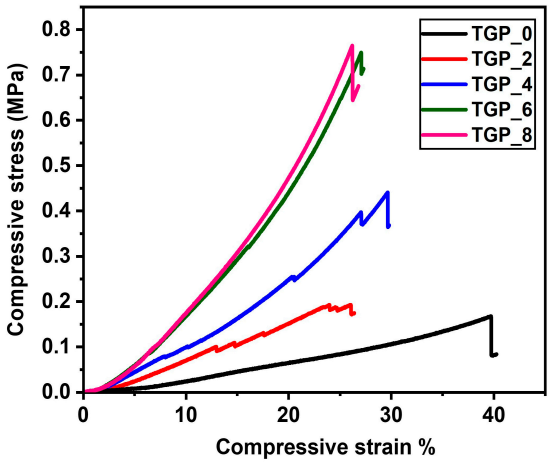

Figure 5. The compressive stress-strain curve of the TGP_X aerogels with varying PACA concentration.

Table 2. The mechanical properties of the TGP_X aerogels with varying PACA concentration.

Aerogel	Breaking Load at 25 % Strain (MPa)	Compressive Modulus (MPa)
TGP_0	0.08	0.4
TGP_2	0.19	0.8
TGP_4	0.36	1.4
TGP_6	0.69	2.7
TGP_8	0.75	2.9

2.5. The Thermal Stability and Performance of the TGP_X Aerogels.

The thermal stability of TGP_X aerogels was studied using Thermogravimetric (TGA) analysis for pristine TGP_0 and hybrid TGP_8 aerogels from 30 to 1000 ^{0}C in a nitrogen atmosphere with a heating rate of 10 ^{0}C min^{-1} for practical insulating applications. The comparative TGA plotting for thermal stability of pristine TGP_0 and hybrid TGP_8 aerogels are shown in Figure 6a. A small initial weight loss (~ 2.5%) occurred with increasing temperature up to 120 ^{0}C, which can be attributed to the evaporation of water molecules, moisture, and persistent organic solvent in the pores of the aerogels. Further, major weight loss observed in second stage, from 315 to 800 ^{0}C due to the decomposition of methyl groups and organic content from GPTMS and PACA polymer in the TGP_X aerogel. Moreover, second-stage decomposition commenced at 315 and 343 ^{0}C for the pristine TGP_0 and hybrid TGP_8 aerogels, respectively, which indicates that the thermal stability of hybrid TGP_X aerogel was increased with addition of thermally stable PACA polymer [55]. Besides, when the temperature was raised to 1000 ^{0}C, a minimal weight loss difference of 1% between the pristine TGP_0 and hybrid TGP_8 aerogels was observed due to the decomposed polymer residue. Therefore, above results endorse that the hybrid TGP_8 aerogel has higher thermal stability than the pristine TGP_0

Preprints (www.preprints.org) | NOT PEER-REVIEWED | Posted: 19 July 2023 doi:10.20944/preprints202307.1321.v1

aerogel, which can be ascribed to the high thermal stability of the silica aerogel and PACA polymer as well as the presence of strong covalent bonding between GPTMS and PACA via epoxy ring-opening polymerization.

To verify the progressive time-dependent thermal insulating performance of the pristine TGP_0 aerogel (diameter of 20 mm and thickness of 21 mm) and hybrid TGP_8 aerogel (diameter of 18 mm and thickness of 19 mm), samples were subjected to a hot plate heated at ~150 ^{0}C and time-dependent IR thermal images was captured as shown in Figure 6b. In the beginning, the pristine TGP_0 aerogel proved its exceptional thermal insulation capability by maintaining a temperature below 35 ^{0}C, even after being placed on a hot plate for 90 seconds. Similarly, the hybrid TGP_8 aerogel placed on a hot plate also showed excellent thermal insulation performance by keeping the temperature below 38 ^{0}C when the time passed for 90 seconds. Thus, these findings illustrate the remarkably similar thermal insulation performances of the pristine TGP_0 and hybrid TGP_8 aerogels, which is attributed to their low thermal conductivity and high thermal stability stemming from the unique mesoporous network structure and hybridization with thermally stable PACA polymer of TGP_X aerogels, respectively.

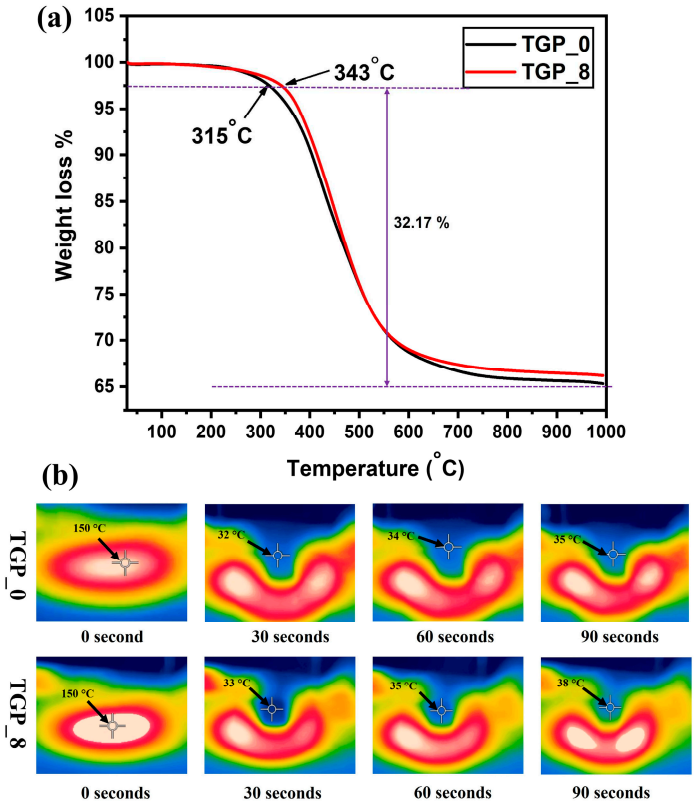

Figure 6. (a) Thermogravimetric analysis (TGA) plots and (b) thermal insulation performances of the pristine TGP_0 and hybrid TGP_8 aerogels: The IR images of the pristine TGP_0 and hybrid TGP_8 aerogels on a hot plate at a temperature of 150 °C viewed from the side.

The hybridized TGP_X aerogels demonstrated better thermal stability as well as an outstanding 7-fold increase in compression modulus compared to the pristine TGP_0 aerogel while maintaining their thermal conductivity values below 30 mW/mK (Figure 7). Such exceptional outcomes of hybrid TGP_X aerogels are credited to the complete hybridization between GPTMS and PACA enhancing the compressive strength of the silica aerogel, which validates the structural reinforcement of hybrid TGP_X aerogels. Meanwhile, the high thermal stability and low thermal conductivity of PACA polymer reward with enhancing thermal stability while maintaining the low thermal conductivity of hybrid TGP_X aerogels. In addition, the fundamental properties of the pristine TGP_0 aerogel, such as density, porosity, and high specific surface area were efficiently maintained in the hybridized TGP_X aerogels. Thus, the selection of PACA as a reinforcing organic polymer is an important part

Preprints (www.preprints.org) | NOT PEER-REVIEWED | Posted: 19 July 2023 doi:10.20944/preprints202307.1321.v1

to synthesize hybridized TGP_X aerogels which showed an outstanding improvement in the mechanical and thermal properties of a silica aerogel which are more beneficial for enhancing its thermal insulation applicability.

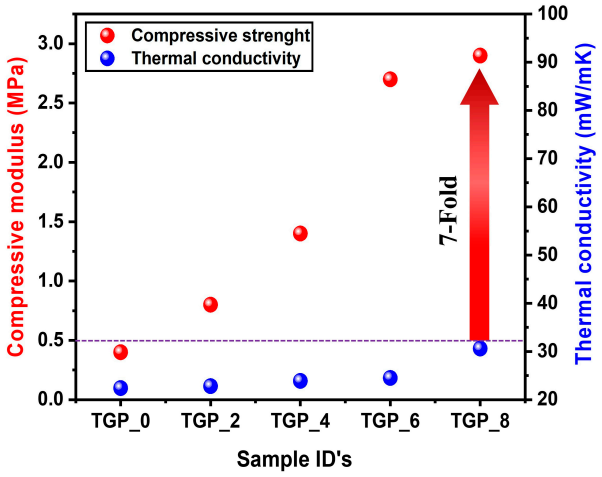

Figure 7. A combined plot of the compression modulus and thermal conductivity of the TGP_X aerogels with varying PACA concentration.

3. Conclusions

Thermally stable and structurally reinforced hybrid TGP_X aerogels were successfully prepared via a facile one-pot sol-gel synthesis method by exploiting epoxy ring-opening polymerization using GPTMS and PACA as a crosslinker and reinforcing polymer, respectively. Although the specific surface area of TGP_X aerogels decreased from 608.6 to 369.0 cm^3/g with increasing polymer content in the aerogel while their porosity and density values were maintained between 95.57% to 93.68% and 0.084 to 0.12 cm^3/g, respectively. Furthermore, the *in-situ* epoxy crosslinking of pristine silica aerogel with PACA polymer reveals outstanding enhancement in the compression modulus, from 0.4 to 2.9 MPa of TGP_X aerogels with maintaining a thermal conductivity from 22.4 to 30.6 mW/mK. In addition, TGA analysis confirms the increase in thermal stability of the hybrid TGP_X aerogel from 315 to 343 ^0C. These results suggest that the epoxy crosslinking between GPTMS and PACA polymer forms a strong covalent bonding that improves the mechanical, thermal, and textural properties of TGP_X aerogels. Conclusively, the facile one-pot synthesis of highly robust and thermally insulating TGP_X aerogel via epoxy ring-opening polymerization using PACA paves a novel way to preparation hybrid aerogels for industrial thermal insulation applications.

4. Materials and Methods

4.1. Materials

The synthesis of the hybrid TGP_X aerogels was carried out by using TMOS ($Si(OCH_3)_4$; 98%) as an Silica precursor, GPTMS ($C_9H_{20}O_5Si$; 98%) as a crosslinker, P(AAm-CO-AAc)) (PACA) as a reinforcing polymer, ammonium fluoride (NH_4F) as a base catalyst, and HCl as an acidic catalyst, all of which were purchased from Sigma-Aldrich. Methanol (Duksan Chemicals) is used as a solvent and deionized (DI) water were used in the experiments. All the chemicals were used as received without any further purification.

4.2. Synthesis of the TGP_X Aerogels

TGP_X aerogels were prepared by using a facile one-pot sol-gel synthesis method, as schematically represented in Figure 8, which consists of pristine TGP and hybrid TPG_X aerogel, explained as follows: Initially, solution A was prepared using a mixture of TMOS, methanol, and DI water to which 0.5 ml of optimized 0.01M HCl was added dropwise as the acidic catalyst for hydrolysis,

Preprints (www.preprints.org) | NOT PEER-REVIEWED | Posted: 19 July 2023 doi:10.20944/preprints202307.1321.v1

followed by 1 hour of stirring at room temperature. Meanwhile, PACA polymer solutions were prepared with different wt% of the polymer (2, 4, 6, and 8 wt%) in DI water. Subsequently, solution B was prepared by using a mixture of GPTMS, methanol, DI water, and PACA polymer solution with different wt%, followed by stirring for 4 hours at room temperature. Then, for hybrid sol-gel synthesis, solution B was added to solution A, followed by vigorously stirring for 1 hour. After allowing an extra 2 hours of hydrolysis, 0.5 ml of 0.1M NH_4F was added as the basic catalyst for condensation, followed by 10 minutes of stirring. For all samples, the gel usually formed within 30 min at 55 ^{0}C. The TGP_X gels were aged in an oven for 3 hours at 55 ^{0}C for further completion of the condensation reaction and to strengthen the gel structure. Monolithic aerogels were obtained through methanol solvent exchange and supercritical alcohol drying (SAD) in (Parr autoclave, USA) at 265 ^{0}C and 120 bar pressure. The preparation of hybrid TGP_X aerogels was performed by using a TMOS: GPTMS: methanol: DI water molar ratio of 1: 0.3: 30: 2, with varying the wt% of PACA polymer solution as 0, 2, 4, 6, and 8 wt% depending upon the solubility of the polymer in methanol. The influence of varying PACA polymer (wt%) on the structural, morphological, and chemical properties and their impact on mechanical strength and thermal stability of TGP_X aerogels was investigated using different types of characterization.

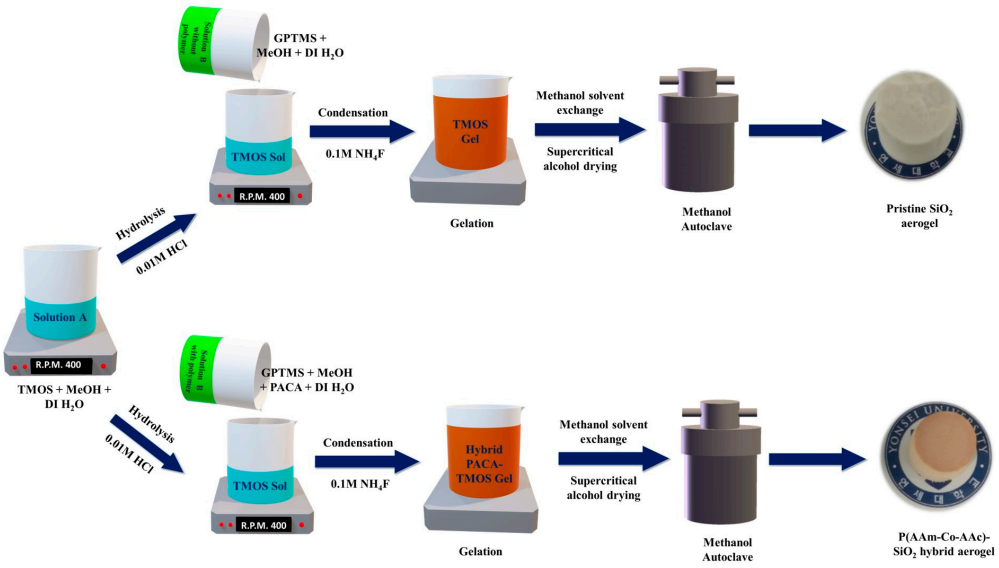

Figure 8. An illustration of one-pot sol-gel synthesis of the pristine TGP_0 and hybrid TGP_X aerogels.

4.3. Characterization of the TGP_X Aerogels

The structural, morphological, chemical, and physical properties of the prepared TGP_X aerogels were investigated by using various characterization techniques. The surface functional group of TGP_X aerogels was examined by using FTIR spectroscopy (PerkinElmer 1760X spectrometer, USA) over a wavelength range from 400 to 4000 cm^{-1}. Chemical crosslinking between GPTMS, PACA, and TMOS was confirmed by using X-ray photoelectron spectroscopy (XPS: K-Alpha, Thermo Fisher Scientific, UK) with a monochromatic Al X-ray source (Al Kα line: 1486.6eV, 3mA, and 12kV). The surface morphologies of the TGP_X aerogels were investigated via field emission scanning electron microscopy (FESEM; JEOL JSM-7001F, Japan) performed at 5–10 kV. Surface area, pore volume, and pore size of TGP_X aerogels were calculated by using the N_2 adsorption-desorption isotherm data obtained from Brunauer-Emmett-Teller (BET) and Barrette-Joyner-Halenda (BJH) analysis (Quantachrome Instruments v10.0). According to previous reports, the bulk density (ϱb) of TGP_X aerogel samples was calculated using the mass-to-volume ratio. The porosity (%) of the TGP_X aerogels were calculated from the reported formula (1) by using ϱs as the skeletal density (~1.9 g/cc) of TGP_X aerogel [36].

The thermal conductivity of TGP_X aerogels was measured by using an ASTM D7984 (Trident-MTPS, C-Therm). Thermogravimetric analysis (TGA: SDT-2790, TA Inc.) was performed to determine the thermal stability temperature of TGP_X aerogel, where measurements carried out in the temperature range of 30 ^{0}C to 1000 ^{0}C with a heating rate of 10 ^{0}C min^{-1}. The mechanical properties of TGP_X aerogels were measured using compressive strength measurements (Shimadzu, Japan, AGX-50kNVD).

Author Contributions: A.A.R.: Conceptualization, Writing-original draft, Software, Formal analysis, Validation, Visualization; R.P.D.: Data curation, Formal analysis, Investigation; V.G.P.: Data curation, Formal analysis, Investigation; U.K.H.: Data curation, Formal analysis, Investigation; H.C.: Data curation, Formal analysis, Investigation; W.L.: Data curation, Formal analysis, Investigation; J.K.: Data curation, Formal analysis, Investigation; Q.W.: Data curation, Formal analysis, Investigation; V.D.P.: Data curation, Formal analysis, Investigation; T.K.: Data curation, Formal analysis, Investigation; W.K.J.: Data curation, Formal analysis, Investigation; H.H.P.: supervision, Project administration, funding acquisition. All authors have read and agreed to the published version of the manuscript.

Funding: This work was supported by the Agency for Defense Development of the Korean Government (Project No.: UI2200411D).

Data Availability Statement: Data will be made available on request.

Conflicts of Interest: The authors declare that they have no known competing financial interest or personal relationships that could have appeared to influence the work reported in this paper.

References

1. A.S. Dorcheh: M. Abbasi. Silica Aerogel; Synthesis, Properties and characterization. *Journal of materials processing technology* **2008**, *199*, 10-26
2. C. Li; Z. Chen; W. Dong; L. Lin; X. Zhu; Q. Liu; Y. Zhang; N. Zhai; Z. Zhou; Y. Wang. A review of Silicon-Based Aerogel Thermal Insulation Materials: Performance Optimization Through Composition and microstructure. *Journal of Non-Crystalline Solids* **2021**, *553*, 120517
3. V.G. Parale; W. Han; K.-Y. Lee; H.-H. Park. Ambient Pressure Dried Tetrapropoxysilane-Based Silica Aerogels With High Specific Surface Area. *Solid State Sciences* **2018**, *75*, 63-70
4. A. Neugebauer; K. Chen; A. Tang; A. Allgeier; L.R. Glicksman; L.J. Gibson. Thermal conductivity and characterization of Compacted, Granular Silica Aerogel. *Energy and buildings* **2014**, *79*, 47-57
5. H. Cai; Y. Jiang; J. Feng; S. Zhang; F. Peng; Y. Xiao; L. Li; J. Feng. Preparation of Silica Aerogels with High Temperature Resistance and Low Thermal Conductivity by Monodispersed Silica Sol. *Materials & Design* **2020**, *191*, 108640
6. M. Koebel; A. Rigacci; P. Achard. Aerogel-Based Thermal Superinsulation: An Overview. *Journal of sol-gel science and technology* **2012**, *63*, 315-339
7. Z. Mazrouei-Sebdani; H. Begum; S. Schoenwald; K.V. Horoshenkov; W.J. Malfait. A review on Silica Aerogel-Based Materials for Acoustic Applications. *Journal of Non-Crystalline Solids* **2021**, *562*, 120770
8. J.E. Amonette; J. Matyáš. Functionalized Silica Aerogels for Gas-Phase Purification, Sensing, and catalysis: A review. *Microporous and Mesoporous Materials* **2017**, *250*, 100-119
9. N. Bheekhun; A. Talib; A. Rahim; M.R. Hassan. Aerogels in aerospace: An Overview. *Advances in Materials Science and Engineering* **2013**, *2013*,
10. X. Zou; K. Liao; D. Wang; Q. Lu; C. Zhou; P. He; R. Ran; W. Zhou; W. Jin; Z. Shao. Water-Proof, Electrolyte-Nonvolatile, and Flexible Li-Air Batteries via O2-Permeable Silica-Aerogel-Reinforced Polydimethylsiloxane External Membranes. *Energy Storage Materials* **2020**, *27*, 297-306
11. A. Lamy-Mendes; A.D.R. Pontinha; P. Alves; P. Santos; L. Durães. Progress in Silica Aerogel-Containing Materials for Buildings' Thermal Insulation. *Construction and Building Materials* **2021**, *286*, 122815
12. J. Kehrle; T.K. Purkait; S. Kaiser; K.N. Raftopoulos; M. Winnacker; T. Ludwig; M. Aghajamali; M. Hanzlik; K. Rodewald; T. Helbich. Superhydrophobic Silicon Nanocrystal–Silica Aerogel Hybrid Materials: Synthesis, Properties, and Sensing Application. *Langmuir* **2018**, *34*, 4888-4896
13. H. Maleki; L. Durães; A. Portugal. Synthesis of Lightweight Polymer-Reinforced Silica Aerogels with Improved Mechanical and Thermal Insulation Properties for Space Applications. *Microporous and Mesoporous Materials* **2014**, *197*, 116-129

14. P. Meti; D. Mahadik; K.-Y. Lee; Q. Wang; K. Kanamori; Y.-D. Gong; H.-H. Park. Overview of Organic–Inorganic Hybrid Silica Aerogels: Progress and perspectives. *Materials & Design* **2022**, 111091
15. J. Lin; G. Li; W. Liu; R. Qiu; H. Wei; K. Zong; X. Cai. A review of Recent Progress on the Silica Aerogel Monoliths: Synthesis, reinforcement, and applications. *Journal of Materials Science* **2021**, *56*, 10812-10833
16. H. Omranpour; S. Motahari. Effects of Processing Conditions on Silica Aerogel During Aging: Role of solvent, time and temperature. *Journal of Non-Crystalline Solids* **2013**, *379*, 7-11
17. L. Zhong; X. Chen; H. Song; K. Guo; Z. Hu. Highly Flexible Silica Aerogels derived from methyltriethoxysilane and polydimethylsiloxane. *New Journal of Chemistry* **2015**, *39*, 7832-7838
18. L. Jiang; K. Kato; K. Mayumi; H. Yokoyama; K. Ito. One-Pot Synthesis and characterization of Polyrotaxane–Silica Hybrid Aerogel. *ACS Macro Letters* **2017**, *6*, 281-286
19. Z. Li; X. Cheng; S. He; X. Shi; L. Gong; H. Zhang. Aramid Fibers Reinforced Silica Aerogel Composites with Low Thermal Conductivity and Improved Mechanical Performance. *Composites Part A: Applied Science and Manufacturing* **2016**, *84*, 316-325
20. W.-C. Hung; R.S. Horng; R.-E. Shia. Investigation of Thermal Insulation Performance of Glass/Carbon Fiber-Reinforced Silica Aerogel Composites. *Journal of Sol-Gel Science and Technology* **2021**, *97*, 414-421
21. Y. Duan; S.C. Jana; B. Lama; M.P. Espe. Self-Crosslinkable Poly (Urethane Urea)-Reinforced Silica Aerogels. *RSC Advances* **2015**, *5*, 71551-71558
22. M.A.B. Meador; A.S. Weber; A. Hindi; M. Naumenko; L. McCorkle; D. Quade; S.L. Vivod; G.L. Gould; S. White; K. Deshpande. Structure− Property Relationships in porous 3D Nanostructures: Epoxy-Cross-Linked Silica Aerogels Produced using ethanol as the solvent. *ACS Applied Materials & Interfaces* **2009**, *1*, 894-906
23. B. Domènech; I. Mata; E. Molins. Tuning the structure and the Mechanical Properties of Epoxy–Silica Sol–Gel Hybrid Materials. *RSC advances* **2016**, *6*, 10736-10742
24. X. Wang; S.C. Jana. Synergistic Hybrid Organic–Inorganic Aerogels. *ACS applied materials & interfaces* **2013**, *5*, 6423-6429
25. Z. Ahmad; J. Mark. Polyimide− Ceramic Hybrid Composites by the Sol− Gel Route. *Chemistry of Materials* **2001**, *13*, 3320-3330
26. H. Maleki; L. Duraes; A. Portugal. Development of Mechanically Strong Ambient Pressure Dried Silica Aerogels with Optimized Properties. *The Journal of Physical Chemistry C* **2015**, *119*, 7689-7703
27. H. Ramadan; A. Ghanem; H. El-Rassy. Mercury removal from Aqueous Solutions using Silica, Polyacrylamide and hybrid Silica–Polyacrylamide Aerogels. *Chemical Engineering Journal* **2010**, *159*, 107-115
28. Q. Wang; H. Yu; Z. Zhang; Y. Zhao; H. Wang. One-Pot Synthesis of Polymer-Reinforced Silica Aerogels From High Internal Phase Emulsion Templates. *Journal of colloid and interface science* **2020**, *573*, 62-70
29. R. Mahon; Y. Balogun; G. Oluyemi; J. Njuguna. Swelling performance of Sodium Polyacrylate and Poly (Acrylamide-Co-Acrylic Acid) Potassium Salt. *SN applied sciences* **2020**, *2*, 1-15
30. T. Linhares; M.T.P. de Amorim; L. Durães. Silica Aerogel Composites with Embedded Fibres: A Review on their Preparation, Properties and applications. *Journal of Materials Chemistry A* **2019**, *7*, 22768-22802
31. S.-N. Zhang; H.-Q. Pang; T.-H. Fan; Q. Ye; Q.-L. Cai; X. Wu. Thermal Insulation Performance of SiC-Doped Silica Aerogels under Large Temperature and Air Pressure Differences. *Gels* **2022**, *8*, 320
32. Z. Yan; Z. Ma; J. Deng; G. Luo. Mechanism and kinetics of Epoxide Ring-Opening with Carboxylic Acids catalyzed by the Corresponding Carboxylates. *Chemical Engineering Science* **2021**, *242*, 116746
33. X. Dai; X. Xu; X. Yu; X. Sun; J. Pan; X. Zhang; J. Min. Cationic Core/Shell Polysiloxane Acrylate Emulsion: Synthesis, Film morphology, and performance on Cotton Pigment Coloration. *Cellulose* **2022**, *29*, 2093-2106
34. S. Zong; W. Wei; Z. Jiang; Z. Yan; J. Zhu; J. Xie. Characterization and comparison of Uniform Hydrophilic/Hydrophobic Transparent Silica Aerogel Beads: Skeleton Strength and Surface Modification. *Rsc Advances* **2015**, *5*, 55579-55587
35. H. Yu; X. Liang; J. Wang; M. Wang; S. Yang. Preparation and characterization of Hydrophobic Silica Aerogel Sphere Products by Co-Precursor Method. *Solid State Sciences* **2015**, *48*, 155-162
36. P. Meti; Q. Wang; Y.-D. Gong; D. Mahadik; H.-H. Park. Sorbitol Cross-Linked Silica Aerogels with Improved Textural and Mechanical Properties. *Ceramics International* **2022**, *48*, 19198-19205
37. V.S. Smitha; P.M.A. Azeez; K.G. Warrier; B.N. Nair; U.N.S. Hareesh. Transparent and Hydrophobic MTMS/GPTMS Hybrid Aerogel Monoliths and Coatings by Sol-Gel Method: A Viable Remedy for Oil-Spill Cleanup. *ChemistrySelect* **2018**, *3*, 2989-2997

38. L. Feng; H. Yang; X. Dong; H. Lei; D. Chen. pH-Sensitive Polymeric Particles as Smart Carriers for Rebar Inhibitors Delivery in Alkaline Condition. *Journal of Applied Polymer Science* **2018**, *135*, 45886
39. T. Prasad; S. Halder; S.S. Dhar. Imidazole-Supported Silica One-Pot Processed Nanoparticles to enhance Toughness of Epoxy Based Nanocomposites. *Materials Chemistry and Physics* **2019**, *231*, 75-86
40. S. Karamikamkar; A. Abidli; E. Behzadfar; S. Rezaei; H.E. Naguib; C.B. Park. The effect of Graphene-Nanoplatelets On Gelation and Structural Integrity of a Polyvinyltrimethoxysilane-Based Aerogel. *RSC advances* **2019**, *9*, 11503-11520
41. H. Choi; T. Kim; T. Kim; S. Moon; S. Yoo; V.G. Parale; R.P. Dhavale; K. Kang; H. Sohn; H.-H. Park. Ultralow Dielectric Cross-Linked Silica Aerogel Nanocomposite Films for Interconnect Technology. *Applied Materials Today* **2022**, *28*, 101536
42. L. Wang; J. Feng; Y. Jiang; S. Zhang; L. Li; J. Feng. Facile fabrication of Hydrophobic Polyvinylpolysilsesquioxane Aerogels with Improved Optical Properties. *Journal of Sol-Gel Science and Technology* **2020**, *94*, 88-97
43. S. Karamikamkar; M. Fashandi; H.E. Naguib; C.B. Park. In situ Interface Design in Graphene-Embedded Polymeric Silica Aerogel with Organic/Inorganic Hybridization. *ACS applied materials & interfaces* **2020**, *12*, 26635-26648
44. W. Zhang; X. Ji; Y. Yin; C. Wang. Temperature Induced Color Changing Cotton Fabricated via grafting Epoxy Modified Thermochromic Capsules. *Cellulose* **2019**, *26*, 5745-5756
45. H. Choi; V.G. Parale; T. Kim; Y.-S. Choi; J. Tae; H.-H. Park. Structural and Mechanical Properties of Hybrid Silica Aerogel formed using Triethoxy (1-Phenylethenyl) Silane. *Microporous and Mesoporous Materials* **2020**, *298*, 110092
46. V.G. Parale; T. Kim; K.-Y. Lee; V.D. Phadtare; R.P. Dhavale; H.-H. Park. Hydrophobic TiO2–SiO2 Composite Aerogels Synthesized via *In Situ* Epoxy-Ring Opening Polymerization and Sol-Gel Process for Enhanced Degradation Activity. *Ceramics International* **2020**, *46*, 4939-4946
47. D. Zhang; J. Xiao; Q. Guo; J. Yang. 3D-Printed Highly Porous and Reusable Chitosan Monoliths for Cu (II) removal. *Journal of Materials Science* **2019**, *54*, 6728-6741
48. A.V. Rao; U.K. Bangi; M.S. Kavale; H. Imai; H. Hirashima. Reduction in the Processing Time of Doped Sodium Silicate Based Ambient Pressure Dried Aerogels using shaker. *Microporous and mesoporous materials* **2010**, *134*, 93-99
49. T.-J. Yim; S.Y. Kim; K.-P. Yoo. Fabrication and Thermophysical Characterization of Nano-Porous Silica-Polyurethane Hybrid Aerogel by Sol-Gel Processing and Supercritical Solvent Drying Technique. *Korean Journal of Chemical Engineering* **2002**, *19*, 159-166
50. M.E. Ghica; C.M. Almeida; M. Fonseca; A. Portugal; L. Durães. Optimization of Polyamide Pulp-Reinforced Silica Aerogel Composites for Thermal Protection Systems. *Polymers* **2020**, *12*, 1278
51. B. Merillas; A. Lamy-Mendes; F. Villafañe; L. Durães; M.Á. Rodríguez-Pérez. Silica-Based Aerogel Composites Reinforced with Reticulated Polyurethane Foams: Thermal and Mechanical Properties. *Gels* **2022**, *8*, 392
52. F. Ilhan; E.F. Fabrizio; L. McCorkle; D.A. Scheiman; A. Dass; A. Palczer; M.B. Meador; J.C. Johnston; N. Leventis. Hydrophobic Monolithic Aerogels by Nanocasting Polystyrene on Amine-Modified Silica. *Journal of Materials Chemistry* **2006**, *16*, 3046-3054
53. H.-N.-R. Jung; Y.K. Lee; V. Parale; H.H. Cho; D. Mahadik; H.-H. Park. Hydrophobic Silica Composite Aerogels using Poly (Methyl Methacrylate) by Rapid Supercritical Extraction Process. *Journal of Sol-Gel Science and Technology* **2017**, *83*, 692-697
54. I.-L. Ngo; S. Jeon; C. Byon. Thermal conductivity of transparent and Flexible Polymers containing fillers: A Literature Review. *International Journal of Heat and Mass Transfer* **2016**, *98*, 219-226
55. M. Zendehdel; A. Barati; H. Alikhani. Preparation and characterization of Poly (Acryl Amide-Coacrylic Acid)/Nay and Clinoptilolite nanocomposites with Improved Methylene Blue Dye Removal Behavior from Aqueous Solution. *e-Polymers* **2011**, *11*,